P-CRESOL ADSORPTION AND HEMOCOMPATIBILITY STUDY ON NANOPOROUS HYDROXYAPATITE

OOI CHEE HEONG

UNIVERSITI SAINS MALAYSIA

2019

P-CRESOL ADSORPTION AND HEMOCOMPATIBILITY STUDY ON NANOPOROUS HYDROXYAPATITE

by

Ooi Chee Heong

Thesis submitted in fulfilment of the requirements for the degree of Doctor of Philosophy

August 2019

ACKNOWLEDGEMENT

First and foremost, I would like to express my gratitude to my supervisor, Assoc. Prof. Dr. Yeoh Fei Yee, who has been given me excellent supervision and guidance in pursuing my doctoral degree. His invaluable help of constructive comments and ideas throughout the experimental and thesis works have contributed to the success of this research. I would like to thank my co-supervisor, Assoc. Prof. Dr. Pung Swee Yong for his guidance and support.

My sincere thanks goes to the respecful Dean, Assoc. Prof. Ir. Dr. Syed Fuad B. Saiyid Hashim and all staff in School of Materials and Mineral Resources Engineering, for providing professional assistance and facilities. Special thanks goes to Prof. Dr. Wan Zaidah Abdullah and Ahmad Zakwan Mustafa for their help and guidance during my research work at Health Campus, USM. I would like to acknowledge the Ministry of Education Malaysia for providing me the financial support through the MyBrain15 scholarship program and necessary fundings for this research through the Prototype Research Grant Scheme (PRGS).

I would like to dedicate my greatest appreciation to my family for supporting and encouraging me in pursuing my doctoral degree. Furthermore, I would like to extend my gratitude to my fellow friends including Cheah Wee Keat, Nur Farahiyah, Lee Ting, Wanie Ismail, Yew Pei Ling, Leong Thye Jien and Chum Yuan Ching for giving me supports and advices when I encountered problems during the research.

TABLE OF CONTENTS

Page

ACKNOWLEDGEMENT ..... **ii**

TABLE OF CONTENTS ..... **iii**

LIST OF TABLES ..... **vii**

LIST OF FIGURES ..... **ix**

LIST OF ABBREVIATIONS ..... **xiii**

LIST OF SYMBOLS ..... **xv**

ABSTRAK ..... **xvi**

ABSTRACT ..... **xviii**

CHAPTER 1 INTRODUCTION **1**

1.1 Research Background 1

1.2 Problem Statement 4

1.3 Research Objectives 7

1.4 Scope of Research 7

1.5 Thesis Outline 9

CHAPTER 2 LITERATURE REVIEW **11**

2.1 Human Kidney and its Function 11

2.1.1 Kidney Failure 12

2.2 Uremic Toxins 14

2.3 Artificial Kidney 17

2.3.1 Hemodialysis 20

2.3.1(a) Dialyzer 23

2.3.1(b) Dialysate 23

2.3.1(c) Limitation of Hemodialysis 24

2.3.2 Artificial Kidney Development 26

2.3.3 Nanoporous Materials for Uremic Toxins Removal 27

2.4 Nanoporous Hydroxyapatite for Uremic Toxins Removal 29

2.4.1 Applications of Nanoporous Hydroxyapatite & Uremic Toxins Removal 30

2.4.2 Pore Characteristics of Nanoporous Hydroxyapatite 31

2.4.3 Synthesis of Nanoporous Hydroxyapatite 33

2.4.3(a) Wet Chemical Reaction 33

2.4.3(b) Templating System 41

2.4.4 Surface Coating of Nanoporous Hydroxyapatite 43

2.5 *In Vitro* Hemocompatibility Evaluation 44

2.5.1 Blood Component and its Functions 45

2.5.2 Hemocompatibility Study on Nanoporous Hydroxyapatite 47

2.6 *p*-Cresol Adsorption 49

2.6.1 Adsorption Isotherm 51

2.6.2 Liquid Phase Adsorption 52

CHAPTER 3 METHODOLOGY 54

3.1 Introduction 54

3.2 Synthesis of Nanoporous Hydroxyapatite 56

3.2.1 Materials and Chemicals 56

3.2.2 Synthesis Process 57

3.2.2(a) Effect of Polyethylene-Polypropylene Unit Ratio of Surfactant 59

3.2.2(b) Effect of Calcination 61

3.2.2(c) Effect of Surfactant Concentration 62

3.2.3 Surface Coating on Nanoporous Hydroxyapatite 63

3.3 Characterization of Nanoporous Hydroxyapatite 65

3.3.1 X-ray Diffraction Analysis 65

3.3.2 Fourier Transform Infrared Spectroscopy 65

3.3.3 Scanning Electron Microscopy and Energy-Dispersive X-ray Spectroscopy 66

3.3.4 Transmission Electron Microscopy 66
3.3.5 Nitrogen Adsorption Analysis 67
3.4 Hemocompatibility Study 67
3.4.1 Hemolysis Test 68
3.4.2 Platelet Adhesion Test 70
3.4.3 Platelet Activation Test 71
3.4.4 Blood Clotting Time Measurement 71
3.4.5 Statistical Analysis 72
3.5 *para*-Cresol Adsorption Test 73
3.5.1 Standard Calibration Curve of *p*-Cresol Solution 73
3.5.2 *p*-Cresol Adsorption Evaluation 76
3.5.3 Adsorption Kinetic Models for *p*-Cresol Removal 77
CHAPTER 4 RESULTS AND DISSCUSION 79
4.1 Introduction 79
4.2 Synthesis and Characterization of Nanoporous Hydroxyapatite 79
4.2.1 Effect of Polyethylene-Polypropylene Unit Ratio 79
4.2.1(a) Phase, Elemental and Chemical Analysis 80
4.2.1(b) Morphological Analysis 84
4.2.1(c) Pore Characteristics 86
4.2.1(d) Proposed Nanoporous Hydroxyapatite Formation 89
4.2.2 Effect of Calcination 91
4.2.2(a) Phase Identification and Chemical Analysis 91
4.2.2(b) Morphological Analysis 94
4.2.2(c) Pore Characteristics 96
4.2.3 Effect of Surfactant Concentration 99
4.2.3(a) Phase Identification and Chemical Analysis 99
4.2.3(b) Morphological Analysis 102
4.2.3(c) Pore Characteristics 104
4.2.4 Effect of Surface Coating on Nanoporous Hydroxyapatite 107
4.2.4(a) Phase Identification and Chemical Analysis 107

4.2.4(b) Morphological Analysis 111
4.2.4(c) Pore Characteristics 114
4.3 Hemocompatibility of Nanoporous Hydroxyapatite 116
4.3.1 Hemolysis Study 116
4.3.2 Platelet Adhesion 120
4.3.3 Platelet Activation 123
4.3.4 Blood Clotting Time 125
4.3.5 Discussion 128
4.4 *p*-Cresol Adsorption by Nanoporous Hydroxyapatite 130
4.4.1 *p*-Cresol Adsorption Kinetics 130
4.4.2 Fitting of Experimental Data onto Adsorption Kinetic Models 134
CHAPTER 5 CONCLUSION AND FUTURE RECOMMENDATIONS ... 141
5.1 Conclusion 141
5.2 Recommendations for Future Research 143
REFERENCES 145
APPENDICES
LIST OF PUBLICATIONS

LIST OF TABLES

Page

Table 1.1	Concentration of *p*-cresol found in healthy person and ESRD patient (Vanholder et al. 2003a; Vanholder et al. 1999)	5
Table 1.2	Criteria of an adsorbent for uremic toxins removal in artificial kidney system (Cheah et al., 2017)	6
Table 2.1	Stages of chronic kidney disease (Peter, 2007)	13
Table 2.2	Concentrations of major uremic toxins measured in healthy persons and ESRD patients (Vanholder et al. 2003a; Vanholder et al. 2003b; Wernert et al. 2005)	15
Table 2.3	Physical properties of *p*-cresol (ATSDR 2008; Wernert et al. 2005)	16
Table 2.4	Synthesis condition and physicochemical properties of nanoporous HA prepared via different wet chemical processes	36
Table 2.5	Comparison of different wet chemical reactions for nanoporous HA synthesis	40
Table 2.6	Comparison between soft and hard-templating system for nanoporous HA synthesis	42
Table 2.7	In vitro hemocompatibility tests for analyzing nanoporous HA samples	48
Table 2.8	Recommended conditions for *in vitro* hemocompatibility test on nanoporous HA samples based on the ISO standard (ISO, 2002)	48
Table 2.9	Differences between the physisorption and chemisorption	51
Table 3.1	List of chemicals used in the synthesis of nanoporous HA	57
Table 3.2	Amount of calcium and phosphate precursors used	59
Table 3.3	Details of non-ionic surfactants used in the synthesis of nanoporous HA	60
Table 3.4	Details of nanoporous HA synthesized with and without calcination	61
Table 3.5	Details of synthesis process in the study of surfactant concentration	62

Table 3.6 Details on the SDS solutions used for coating on the nanoporous HA 64
Table 3.7 Details on all nanoporous HA samples synthesized in this project ... 64
Table 4.1 Particle size measurement for nanoporous HA based on the transmission electron micrographs (each value is presented as mean of 10 measurements) 86
Table 4.2 Pore characteristics of synthesized nanoporous HA 88
Table 4.3 Particle size measurement for nanoporous HA based on the transmission electron micrographs (each value is presented as mean of 10 measurements) 96
Table 4.4 Pore characteristics of synthesized nanoporous HA samples 99
Table 4.5 Particle size measurement for HA-P, HA-P12 and HA-P24 based on the transmission electron micrographs (each value is presented as mean of 10 measurements) 104
Table 4.6 Pore characteristics of nanoporous HA prepared with different surfactant concentration 106
Table 4.7 Particle size measurement for SDS-coated nanoporous HA samples based on the transmission electron micrographs (each value is presented as mean of 10 measurements) 113
Table 4.8 Pore characteristics of SDS-coated nanoporous HA samples 115
Table 4.9 Pseudo-first order and pseudo-second order kinetic model for *p*-cresol adsorption by nanoporous HA ($q_{e,exp}$ experimental, mg/g ; q_e, mg/g; k_1,1/min ; k_2, g/(mg min)) 135

LIST OF FIGURES

Page

Figure 1.1	Project outline	10
Figure 2.1	Schematic diagram of human kidney and nephron (modified from Nephron Kidney Glomerulus Renal Cortex Osmoregulation PNG, 2019)	12
Figure 2.2	ESRD treatment modality (Health, 2011)	18
Figure 2.3	Schematic diagram of peritoneal dialysis	19
Figure 2.4	Schematic diagram of a present hemodialysis (Jèorres et al., 2010)	21
Figure 2.5	Schematic diagram of a dialyzer	21
Figure 2.6	Dialyzer used in a hemodialysis treatment (Fresenious Medical Care)	22
Figure 2.7	Percentage of *p*-cresol removed by hemodialysis	25
Figure 2.8	Utilization of nanoporous HA in a hemodialysis based artificial kidney system	29
Figure 2.9	Schematic cross-section of a nanoporous material (Rouquerol et al., 1994)	32
Figure 2.10	Categorized nanoporous materials based on the IUPAC classification and ISO nanoporous classification	33
Figure 2.11	Schematic diagram of the steps involved in the chemical precipitation and hydrothermal processes	35
Figure 2.12	(a) SEM and (b) TEM images of carbonated HA synthesized via hydrothermal soft-templating method (Mohammad et al., 2015)	43
Figure 2.13	Chemical structure of sodium dodecyl sulfate	44
Figure 2.14	Blood components and its percentage by volume	45
Figure 2.15	Blood cells and its functions	46
Figure 2.16	Shematic diagram of a surface phenomenon in an adsorption process	49
Figure 2.17	Types of physisorption isotherms (Pierotti and Rouquerol, 1985)	52
Figure 3.1	Flowchart of the research methodology	55

Figure 3.2 Flowchart for nanoporous HA synthesis process 58
Figure 3.3 Calibration curve of *p*-cresol solution at characteristic peak ranged between 275-300 nm 75
Figure 3.4 Linear calibration curve of *p*-cresol solution at characteristic peak ranged between 275-300 nm 75
Figure 4.1 X-ray diffractograms of HA-P-C, HA-F-C and HA-0..... 81
Figure 4.2 Qualitative elemental analysis of nanoporous HA by using energy dispersive spectroscopy (EDS)..... 82
Figure 4.3 Fourier transform infrared spectra of surfactants (Pluronic P123 and F127), nanoporous HA and control samples 83
Figure 4.4 SEM images of (a) HA-P-C and (b) HA-F-C at 30,000× magnification..... 84
Figure 4.5 Transmission electron micrographs of HA-P-C and HA-F-C at the size scales of (a) 50 nm (b) 20 nm 86
Figure 4.6 N_2 adsorption isotherms of HA-P-C, HA-F-C and HA-0 at -196 ˚C 87
Figure 4.7 Pore size distribution by BJH method for HA-P-C, HA-F-C and HA-0 87
Figure 4.8 (a) Formation of nanoporous HA based on surfactant-templating system and (b) hydrogen bonding formed between micelle and Ca precursor..... 90
Figure 4.9 X-ray diffractograms of HA-P-C and HA-P samples..... 92
Figure 4.10 Fourier transform infrared spectra of Pluronic P123 and nanoporous HA samples 94
Figure 4.11 SEM images of HA-P at (a) 10000× and (b) 30000× magnification..... 95
Figure 4.12 Transmission electron micrographs of HA-P-C and HA-P at the size scales of (a) 50 nm (b) 20 nm..... 95
Figure 4.13 N_2 adsorption isotherms of HA-P-C and HA-P samples 97
Figure 4.14 (a) Pore size distribution by BJH method for HA-P-C and HA-P samples and (b) schematic diagram on the porosity formed in the nanoporous HA..... 98
Figure 4.15 X-ray diffractograms of HA-P, HA-P12 and HA-P24 samples 100

Figure 4.16 Fourier transform infrared spectra of P123 and nanoporous HA samples prepared from different surfactant concentration 102
Figure 4.17 SEM images of HA-P12 and HA-P24 at (a) 10000× and (b) 30000× magnification 103
Figure 4.18 Transmission electron micrographs of HA-P12 and HA-P24 at the size scales of (a) 50 nm and (b) 20 nm 103
Figure 4.19 N_2 adsorption isotherms of nanoporous HA samples prepared with different surfactant concentrations 105
Figure 4.20 Pore size distribution by BJH method for nanoporous HA samples prepared with different surfactant concentrations 106
Figure 4.21 X-ray diffractograms of SDS-coated nanoporous HA samples 108
Figure 4.22 Fourier transform infrared spectra of SDS and SDS-coated nanoporous HA samples at (a) 4000-400 cm^{-1} and (b) 3100-2700 cm^{-1} 110
Figure 4.23 SEM images of (a) HA-P24, (b) HA-P24-S1, (c) HA-P24-S2, (d) HA-P24-S4, (e) HA-P24-S6 and (f) HA-P24-S8 at 10000× magnification 111
Figure 4.24 Transmission electron micrographs of (a) HA-P24, (b) HA-P24-S1, (c) HA-P24-S2, (d) HA-P24-S4, (e) HA-P24-S6 and (f) HA-P24-S8 at the size scales of 20 nm 112
Figure 4.25 N_2 adsorption isotherms of SDS-coated nanoporous HA samples .. 114
Figure 4.26 Pore size distribution by BJH method for SDS-coated nanoporous HA samples 115
Figure 4.27 Percentage of hemolysis of nanoporous HA samples prepared from (a) surfactants with different PEO-PPO unit ratio, (b) with and without going through calcination(c) different surfactant concentration and (d) SDS coating 117
Figure 4.28 Percentage of platelet adhesion of (a) collagen-coated glass, silicone tube and nanoporous HA prepared from different surfactants, (b) nanoporous HA prepared with and without calcination process (c) different surfactant concentration and (d) SDS-coated HA samples 121
Figure 4.29 Schematic diagram for five-point scale of increasing degree of platelet activation (Goodman, 1999) 123

Figure 4.30 Morphology of platelets adhered on (a) collagen-coated glass and (b) silicone tube, (c) HA-P-C and (d) HA-F-C (12,000× magnification)..... 124
Figure 4.31 Blood clotting time measurement for (a) glass, baseline and nanoporous HA prepared from different surfactant, (b) uncalcined nanoporous HA, (c) different surfactant concentrations and (d) SDS-coated HA samples..... 126
Figure 4.32 Absorbance of *p*-cresol solution before and after exposure to nanoporous HA for (a) 4 minutes, (b) 60 minutes and (c) 240 minutes..... 131
Figure 4.33 *p*-Cresol adsorption kinetics of nanoporous HA samples synthesized via (a) different surfactants, (b) without calcination (c) via various surfactant concentrations and (d) coated with SDS. 132
Figure 4.34 Pseudo second order kinetic model for *p*-cresol adsorption by nanoporous HA synthesized via (a) different surfactant, (b) without calcination, (c) various surfactant concentrations and (d) nanoporous HA coated with SDS..... 136
Figure 4.35 *p*-Cresol adsorption capacity (calculated from pseudo second order kinetic model) of nanoporous HA samples synthesized via different parameters and SDS coating 140

LIST OF ABBREVIATIONS

ANOVA	Analysis of Variance
ARF	Acute Renal Failure
BET	Brunauer–Emmett–Teller
BJH	Barrett-Joyner-Halenda
BUN	Blood Urea Nitrogen
$CaCl_2$	Calcium Chloride
CKD	Chronic Kidney Disease
CMC	Critical Micelle Concentration
CO_2	Carbon Dioxide
C_M	Maximum uremic concentration
C_U	Mean concentration of uremic toxins in patients' body
C_H	Normal / healthy uremic concentration
DI	Deionized water
EDS	Energy Dispersive X-ray
ESEM	Environmental Scanning Electron Microscopy
ESRD	End-Stage Renal Disease
EUTox	European Uremic Toxin Workgroup
FESEM	Field Emission Scanning Electron Micrscopy
FTIR	Fourier Transform Infrared
FWHM	Full Width Half Maximum
HA	Hydroxyapatite
HRTEM	High Resolution Transmission Electron Microscopy
ICDD	International Centre of Diffraction Data
IUPAC	International Union of Pure and Applied Chemistry
K2EDTA	Dipotassium Ethylenediaminetetraacetic Acid
KBr	Potassium Bromide
N_2	Nitrogen
NaOH	Sodium Hydroxide

p-Cresol	*para*-Cresol
PBS	Phosphate Buffer Saline
PEO	Polyethylene Oxide
PPO	Polypropylene Oxide
PPP	Plasma Poor Platelet
PRP	Plasma Rich Platelet
PSD	Pore Size Distribution
RRT	Renal Replacement Therapy
SDS	Sodium Dodecyl Sulphate
SEM	Scanning Electron Microscopy
TEM	Transmission Electron Microscopy
UV-Vis	Ultraviolet-Visible
WAK	Wearable Artificial Kidney
XRD	X-ray Diffractometry

LIST OF SYMBOLS

2θ	Angle of Diffraction
%	Percentage
wt %	Weight Percent
^{o}C	Unit of Temperature in Celcius Scale
K	Unit of Temperature in Kelvin Scale
g	Gram
k_1	Pseudo first Order Rate Constant
k_2	Pseudo Second Order Rate Constant
kg	Kilogram
L	Liter
m	Meter
ml	Mililiter
mg	Miligram
nm	Nanometer
q_t	*p*-Cresol adsorption capacity at time t
q_e	*p*-Cresol adsorption capacity determined from kinetic model
$q_{e,exp}$	*p*-Cresol adsorption capacity determined from experiment

PENJERAPAN *P*-CRESOL DAN KAJIAN KESERASIAN DARAH TERHADAP HIDROKSIAPATIT BERLIANG NANO

ABSTRAK

Sistem hemodialisis semasa tidak dapat menyingkirkan toksin uremik (terutamanya *p*-cresol) secara berkesan dan ini telah menjejaskan kesihatan pesakit dialisis. Oleh itu, prestasi proses dialisis harus dipertingkatkan melalui penggunaan media penjerap untuk penyingkiran *p*-cresol dalam sistem dialisis. Hidroksiapatit (HA) berliang nano merupakan bahan penjerap yang berpotensi untuk digunakan dalam penyingkiran *p*-cresol kerana ia mempunyai biokeserasian yang baik dan liang nano yang boleh dibentuk melalui proses sintesis. Objektif projek ini adalah menghasilkan HA berliang nano bagi aplikasi penyingkiran *p*-cresol dan menilai keserasian darah terhadap bahan tersebut. HA berliang nano telah disintesis melalui kaedah hidroterma menggunakan surfaktan bukan ionik sebagai templat untuk mewujudkan liang dalam bahan tersebut. Kesan surfaktan dengan unit polietilena oksida-polipropelena oksida (PEO-PPO) yang berbeza (iaitu P123 dan F127), pengkalsinan dan kepekatan surfaktan terhadap ciri-ciri liang daripada HA berliang nano telah disiasat. Natrium dodesil sulfat (SDS) yang berlainan kepekatan telah disalutkan pada HA berliang nano untuk meningkatkan kadar penyingkiran *p*-cresol melalui interaksi hidrofobik. Penggunaan Pluronic P123 dan F127 sebagai templat dalam sintesis telah menghasilkan partikel HA yang berbentuk rod. Ia telah meningkatkan luas permukaan HA berliang nano sebanyak 21-59 % berbanding dengan HA yang disintesis tanpa surfaktan. Partikel-partikel HA dengan nisbah aspek (nisbah panjang-ke-diameter) yang tinggi dan luas permukaan yang lebih lebar telah dihasilkan tanpa pengkalsinan dalam proses sintesis. Penggunaan surfaktan

yang berkepekatan lebih tinggi (12 dan 24 mmol/L) telah menghasilkan HA berliang nano dengan ciri-ciri liang yang lebih baik. SDS berjaya disalutkan pada HA berliang nano apabila kepekatannya ditetapkan pada 1 dan 2 mmol/L. Keserasian darah terhadap HA berliang nano dinilai melalui ujian hemolisis, lekatan platelet, pengaktifan platelet dan pengukuran masa pembekuan darah. Keputusan kajian ini menunjukkan bahawa HA berliang nano adalah bahan berserasi darah dan ia tidak mendatangkan sebarang kesan negatif kepada sel-sel darah. Penjerapan *p*-cresol dilakukan untuk menilai kapasiti penjerapan HA berliang nano yang disintesis melalui parameter yang berbeza. HA berliang nano dengan luas permukaan tinggi telah menunjukkan kapasiti penjerapan yang amat baik. Ciri-ciri liang merupakan faktor penting yang menpengaruhi prestasi penjerapan HA berliang nano. Penyalutan SDS telah meningkatkan kadar penyingkiran *p*-cresol oleh HA berliang nano. Penjerapan *p*-cresol terbaik ditunjukkan oleh HA berliang nano yang disintesis menggunakan P123 dengan kepekatan 24 mmol/L tanpa pengkalsinan dan disalutkan dengan SDS (kepekatan 4 mmol/L), ia dilabel sebagai HA-P24-S4. Sampel tersebut menunjukkan kadar penjerapan *p*-cresol sebanyak 2.45 mg/g.

P-CRESOL ADSORPTION AND HEMOCOMPATIBILITY STUDY ON NANOPOROUS HYDROXYAPATITE

ABSTRACT

The present hemodialysis system is ineffective in removing protein-bound uremic toxins, particularly *para*-cresol (*p*-cresol) which seriously affects dialysis patients' health. Thus, it is vital to improve the dialysis process by introducing an effective adsorbent for *p*-cresol removal in artificial kidney system. Nanoporous hydroxyapatite (HA) is a potential biomaterial for *p*-cresol removal in artificial kidney system due to its excellent biocompatibility and porosity, which can be optimized via HA synthesis. This study aimed to synthesize nanoporous HA with well-developed porosity and good hemocompatibility targeted for *p*-cresol removal application. Nanoporous HA was synthesized via hydrothermal method using non-ionic surfactant as soft templates to introduce pores into the biomaterial. The effects of surfactant with different polyethylene-polypropylene (PEO-PPO) unit ratio (i.e., P123 and F127), calcination and surfactant concentration on the pore characteristics of nanoporous HA were investigated. Sodium dodecyl sulfate (SDS) of different concentrations were coated on nanoporous HA as hydrophobic layer to improve the *p*-cresol removal via hydrophobic interaction. The use of Pluronic P123 and F127 as soft templates in HA synthesis process yielded rod-like HA particles, which agglomerated to form pores. This synthesis method improved the BET surface area of nanoporous HA by 21- 59 % while maintaining the HA phase. The absence of calcination in synthesis process produced HA particles with higher surface area and aspect ratio (length-to-diameter). The increase of surfactant (Pluronic P123) concentration from 6 to 12 and 24 mmol/L resulted in nanoporous HA with better

pore characteristics which were desired for achieving a higher *p*-cresol adsorption capacity. SDS was successfully coated on nanoporous HA at the concentration of 1 and 2 mmol/L. The hemocompatibility of the biomaterial was evaluated via hemolysis test, platelet adhesion, platelet activation and blood clotting time measurement. The results reveal that nanoporous HA is a highly hemocompatible biomaterial and it does not induce any change to blood cells when they are in contact, indicating the feasibility of utilizing the biomaterial in artificial kidney application. *p*-Cresol adsorption performance was evaluated for nanoporous HA synthesized via different parameters. Nanoporous HA with a larger surface area exhibited better *p*-cresol adsorption capacity as compared to HA sample with a lower surface area. Pore characteristics are the decisive factors that affect the adsorption performance of nanoporous HA. The SDS coating enhanced the rate constant of *p*-cresol removal by nanoporous HA. The best *p*-cresol adsorption performance is shown by nanoporous HA synthesized using P123 at the concentration of 24 mmol/L without going through calcination process and coated with SDS (concentration 4 mmol/L), which is designed as HA-P24-S4 with a *p*-cresol uptake of 2.45 mg/g.

CHAPTER 1

INTRODUCTION

1.1 Research Background

Nanoporous materials are solid matters that comprise an enormous amount of pores with the pore size less than 100 nm (Polarz and Smarsly, 2002). They have a high surface area and versatile surface properties, which are very useful for applications like separation, sensing, chromatography and catalysis (Lu and Zhao, 2004). Activated carbon, zeolites and mesoporous silica are typical examples of nanoporous materials. These materials have been used as adsorbents in applications such as wastewater treatment, air purification (Bandosz, 2006), gas storage (Morris and Wheatley, 2008) and heavy metal adsorption (Santasnachok et al., 2015, Zare-Dorabei et al., 2016).

Nanoporous materials with excellent pore characteristics (surface area and pore volume) and adsorption capability are preferred biomaterials for many biomedical applications. For instance, activated carbon is a common adsorbent utilized in water purification (Phan et al., 2006) and hemoperfusion treatment (Rosiński et al., 2004). Zeolites and mesoporous silica are used as a carrier for drugs, i.e., chloroquine (Hayakawa et al., 2000), anthelmintic (Dyer et al., 2000), camptothecin (Lu et al., 2007) and antibiotics (Cerri et al., 2004, Ehlert et al., 2011). Hydroxyapatite (HA) is another typical example of biomaterial which is very important in the scaffolding for bone tissue engineering (Pal and Pal, 2006, Woodard et al., 2007).

HA has a composition similar to bone tissue with better bioactivity, biocompatibility and osteoconductivity as compared to the other biomaterials (Swain

and Sarkar, 2013). Nanoporous HA is used for drug delivery (Zhao et al., 2011), protein and nucleic acids fractionation (Sharpe et al., 1997, Tiselius et al., 1956) due to its good protein affinity and porosity (Sharpe et al., 1997, Zhao and Ma, 2005). The excellent biocompatibility and porosity indicate that nanoporous HA can be used as an adsorbent in the present hemodialysis system to improve the efficiency of uremic toxins removal.

Hemodialysis is a preferred renal replacement therapy for patients suffering from kidney failure. The typical dialysis treatment removes toxins from a patient's blood via diffusion through a semipermeable membrane into dialysis fluid or commonly known as dialysate (Debowska et al., 2011). Patients suffer from permanent kidney failure or end-stage renal disease (ESRD) need to undergo hemodialysis treatment to remove wastes from their blood and maintain the electrolytes balance.

Present hemodialysis treatment is unable to fully mimic the functions of a healthy human kidney and has several major drawbacks. One of the limitations is its ineffectiveness in removing protein-bound uremic toxins such as *para*-cresol (*p*-cresol) and indoxyl sulfate (Wernert et al., 2005, Cheng et al., 2018). The uremic toxins which are not removed would gradually accumulate in patients' body and bring about harmful effects. For instance, the retention of *p*-cresol in dialysis patients' body could cause respiratory failure, nervous disorder and mortality (De Smet et al., 1998, Dou et al., 2002). Besides, the hemodialysis treatment required a large amount of dialysate. Approximately 100 L of filtered water is needed to prepare fresh dialysate for a typical dialysis treatment (Tong et al., 2001). It is not efficient in term of water usage, causing the design of a hemodialysis machine to be

bulky. The constant supply of filtered water to a dialysis machine during hemodialysis treatment has restricted the miniaturization of the dialysis system. Dialysis patients have to be static and attached to a dialysis machine throughout the hemodialysis treatment. The polymeric membrane, paticularly polysulfone used in hemodialysis machine showed poor hemocompatibility (Barzin et al., 2004) and released bisphenol A (BPA) into dialysis patients' blood which could cause cardiovascular diseases (Bosch-Panadero et al., 2016).

During hemodialysis treatment, patients are connected to a dialysis machine for about 4 hours per session and the procedure is repeated 3 times per week (Obi et al., 2016). This has significantly affected their freedom and mobility. On top of that, patients without an adequate and versatile working hour may be facing a risk for job loss due to their needs to undergoing hemodialysis treatment at a dialysis center. The collective impact would eventually affect the productivity of the national workforce. A long term hemodialysis treatment will be a heavy financial burden for patients and to the national health care system. Generally, it caused about RM 190 per hemodialysis treatment (Bavanandan et al., 2016). Dialysis treatment is a painful process as it caused physical suffering and mental stress to patients (Cukor et al., 2013). The patients are prone to depression due to the drastic change in their daily routine and activities. For example, they have to give up full-time jobs, family activities or travel to receive frequent dialysis treatment at designated hemodialysis centers.

An ideal artificial kidney with efficient uremic toxins removal is needed by dialysis patients to restore their health and improve the quality of lives. The efficiency of the present hemodialysis system could be enhanced by the introduction

of nanoporous HA as an adsorbent to remove uremic toxins, particularly *p*-cresol via adsorption process.

1.2 Problem Statement

The present hemodialysis treatment is incapable of removing protein-bound uremic toxin, especially *p*-cresol effectively and it affected dialysis patients' health. The retention of the protein-bound uremic toxin in dialysis patients' bodies could result in adverse effects such as inhibition of platelet activating factor synthesis (Wratten et al., 1999) and reduction of endothelial cell response to inflammatory cytokines (Dou et al., 2002). The hemodialysis treatment can only eliminate only 29-38 % of *p*-cresol during a dialysis treatment which is relatively low compared to the removal of other low molecular weight solutes such as urea (75.5 %) and creatinine (66.6 %) (Lesaffer et al., 2000).

The concentration of *p*-cresol found in ESRD patient is about 30 times larger than that of a healthy person as shown in Table 1.1. This uremic toxin presents in the form of protein-bound *p*-cresol (90 %) and free *p*-cresol (non-protein bound, 10 %) in ESRD patients' body. Such a fraction of free *p*-cresol is not observed in a healthy person which contains more than 99 % protein-bound *p*-cresol (Vanholder et al., 2003a). Even though occupying a smaller percentage in the human body, the retention of free *p*-cresol can induce serious problems to dialysis patients i.e., mortality (Bammens et al., 2006) and cardiovascular disease (Meijers et al., 2008) as compared to its protein-bound constituent. Thus, it is vital to enhance the removal of the targeted uremic toxins in the dialysis system. The efficiency of uremic toxins (particularly *p*-cresol) removal could be improved via the introduction of nanoporous HA as an adsorbent into the present hemodialysis system.

Table 1.1 Concentration of *p*-cresol found in healthy person and ESRD patient (Vanholder et al. 2003a; Vanholder et al. 1999)

Property	Healthy person	ESRD patient
Concentration of *p*-cresol in body (µmol/L)	6	186-376
Percentage of protein-bound *p*-cresol (%)	> 99	90
Percentage of free *p*-cresol (%)	≈ 0	10

There are several important criteria to be met when applying an adsorbent into an artificial kidney system i.e., effective removal of all types of uremic toxins, hemocompatible and non-toxic (Table 1.2). Based on the criteria, nanoporous HA is a potential adsorbent for the uremic toxins removal due to its extraordinary biocompatibility, protein affinity and well-developed porosity (Puvvada et al., 2010, Moeller-Siegert et al., 2013, Kandori et al., 2014). HA exhibits excellent bioactivity, osteoconductivity and hemocompatibility as compared to the other porous materials such as activated carbon, activated alumina, mesoporous silica and zeolites (Singh, 2012, Radha et al., 2015). HA shows good protein affinity due to the interaction between calcium-binding sites (HA) and carboxyl groups of protein (Bolander et al., 1988), hence it is used in chromatography for protein fractionation and adsorption (Yin et al., 2002, Fujii et al., 2006, Cleland and Vashishth, 2015). The excellent protein affinity suggests that nanoporous HA is an effective adsorbent for removing the protein-bound uremic toxins, specifically *p*-cresol.

Nanoporous HA with a pore size greater than that of the *p*-cresol molecular size (0.66×0.76×0.39 nm) and large pore volume is needed for the effective uremic toxin removal (Wernert et al., 2006). An ideal pore size for the nanoporous HA is hypothsized to be at least 1.52 nm (double the molecular size of *p*-cresol) to allow

the occurrence of bilayer or multilayer adsorption by the biomaterial. The porosity of nanoporous HA could be developed via hydrothermal soft-templating (using surfactant) synthesis method to achieve a higher *p*-cresol adsorption capacity. For instance, surfactant (e.g., Pluronic F127) is used as a soft template for HA synthesis process to form a porous structure (Zhao and Ma, 2005) and it has significantly improved the adsorption capacity of the biomaterial (Ye et al., 2010). By cross referencing to the synthesis of mesoporous silica, hydrothermal technique facilitate the interaction of HA with surfactant which formed micelles and act as nanoporous templates compared to other wet chemical methods, i.e., chemical precipitation and emulsion (Sadat-Shojai et al., 2012).

Table 1.2 Criteria of an adsorbent for uremic toxins removal in artificial kidney system (Cheah et al., 2017)

Criterion	Remarks
Effective removal of all types of uremic toxins	Particularly *p*-cresol which is not effectively removed by hemodialysis
Highly hemocompatible	To prevent damage to blood cells
Non-toxic	To prevent toxification to patients

The utilization of the developed nanoporous HA in hemodialysis system could enhance the effectiveness of uremic toxins removal, regenerate dialysate, decrease the operating cost and miniaturize the design of dialysis machine (making it into a portable or wearable dialysis machine). This project is intended to explore the feasibility of applying nanoporous HA as an effective adsorbent for uremic toxins removal, thus improving quality of lives for dialysis patients through design enhancement of the present hemodialysis system.

1.3 Research Objectives

This research is aimed to explore the feasibility of improving the efficiency of uremic toxins removal in the present hemodialysis system via adsorption by nanoporous HA. Research objectives of this project are:

1. To synthesize nanoporous HA via hydrothermal soft templating method and to investigate the effect of various synthesis parameters on the physicochemical properties of the biomaterial.
2. To introduce a hydrophobic layer on nanoporous HA via sodium dodecyl sulfate (SDS) coating and to investigate its effect on the physicochemical properties of the biomaterial.
3. To evaluate the *in vitro* hemocompatibility of nanoporous HA and to determine the feasibility of using the biomaterial in the hemodialysis application.
4. To evaluate the *p*-cresol adsorption performance of nanoporous HA.

1.4 Scope of Research

In this study, nanoporous hydroxyapatite (HA) was synthesized by a hydrothermal method using non-ionic surfactant (Pluronic P123 and F127) as a soft template to develop porous structure in the biomaterial. The use of the surfactants in this synthesis process could produce HA sample with nanoporous structure while maintaining the HA phase (Mohammad et al., 2015). Several synthesis parameters were studied to improve the pore characteristics and adsorption capacity of the nanoporous HA i.e., polyethylene-polypropylene (PEO-PPO) unit ratio of surfactant, calcination, surfactant concentration and hydrophobic surface coating. By studying these parameters, the pore characteristics and surface functional groups of the

nanoporous HA could be optimized to achieve desired *p*-cresol adsorption performance.

The synthesized samples were examined through various characterization techniques to verify a successful synthesis of nanoporous HA. X-ray diffraction (XRD) analysis and Fourier transform infrared (FTIR) spectroscopy were used to determine the HA phase. Meanwhile, the morphology of the nanoporous HA was observed using scanning electron microscope (SEM) and transmission electron microscope (TEM). The effects of the synthesis parameters on the pore characteristics and adsorption property of the nanoporous HA were investigated via nitrogen adsorption analysis.

In vitro hemocompatibility study was conducted to determine the compatibility and feasibility of applying nanoporous HA in biomedical applications especially hemodialysis. The i*n vitro* hemocompatibility evaluation of nanoporous HA was carried out through hemolysis test, platelet adhesion, platelet activation and blood clotting time measurement. These tests could determine the physical change in red blood cells and platelets when they are in contact with nanoporous HA. A hemocompatible biomaterial is not expected to induce any physical change to blood components.

Finally, *p*-cresol adsorption test was performed to evaluate the adsorption capability of nanoporous HA prepared from selected synthesis parameters. The concentration of the *p*-cresol solution used for adsorption kinetics study was fixed at 200 µmol/L, mimicking the concentration measured in ESRD patients' blood (Wernert et al., 2006). The duration was set at 4 hours which is corresponding to the typical time of a hemodialysis treatment. The setting of these conditions was to

simulate the patient's body condition during the dialysis process. The effectiveness of utilizing nanoporous HA for *p*-cresol removal was determined based on the adsorption capacity and kinetics.

1.5 Thesis Outline

This thesis is separated into five chapters to explain the whole research in detail. The outline of the project is shown in Figure 1.1. Chapter 1 provides a general introduction on nanoporous materials used for adsorption applications, limitations of present hemodialysis system, specific requirements of applying an adsorbent in dialysis process and utilization of nanoporous material in dialysis system for effective uremic toxins removal. Research background, problem statement, objectives and scope of the research are presented in this chapter.

Chapter 2 summarizes the renal replacement therapies available to ESRD patients, technical issues related to the present dialysis system, development of portable artificial kidney and the improvement in dialysis efficiency via adsorption by nanoporous material. The criteria on the selection of nanoporous HA as an adsorbent for uremic toxins removal, material synthesis process and the importance of *in vitro* hemocompatibility evaluation on biomaterials are also discussed in this chapter.

Chapter 3 reports on the chemicals and selected synthesis method used for the preparation of nanoporous HA as well as details on materials characterization techniques performed. *In vitro* hemocompatibility examination on nanoporous HA is elaborated. The experimental procedures for *p*-cresol adsorption evaluation are also presented.

Chapter 4 contains the technical discussion on the physicochemical properties of nanoporous HA prepared from selected synthesis parameters. The properties that would directly affect the *p*-cresol adsorption capacity of nanoporous HA i.e., pore characteristics and surface functional group were analyzed. The *in vitro* hemocompatibility evaluation for nanoporous HA was performed through hemolysis test, platelet adhesion, platelet activation and blood clotting time measurement. The results from these studies were analyzed to determine the compatibility and feasibility of utilizing nanoporous HA in hemodialysis application. The *p*-cresol adsorption kinetics and capacity of nanoporous HA were evaluated to determine the effectiveness of using the biomaterial for uremic toxins removal.

Finally, Chapter 5 presents the conclusion of the important findings in this project. This chapter also includes recommendations for future work and possible improvements to be carried out in this specific field for the near future.

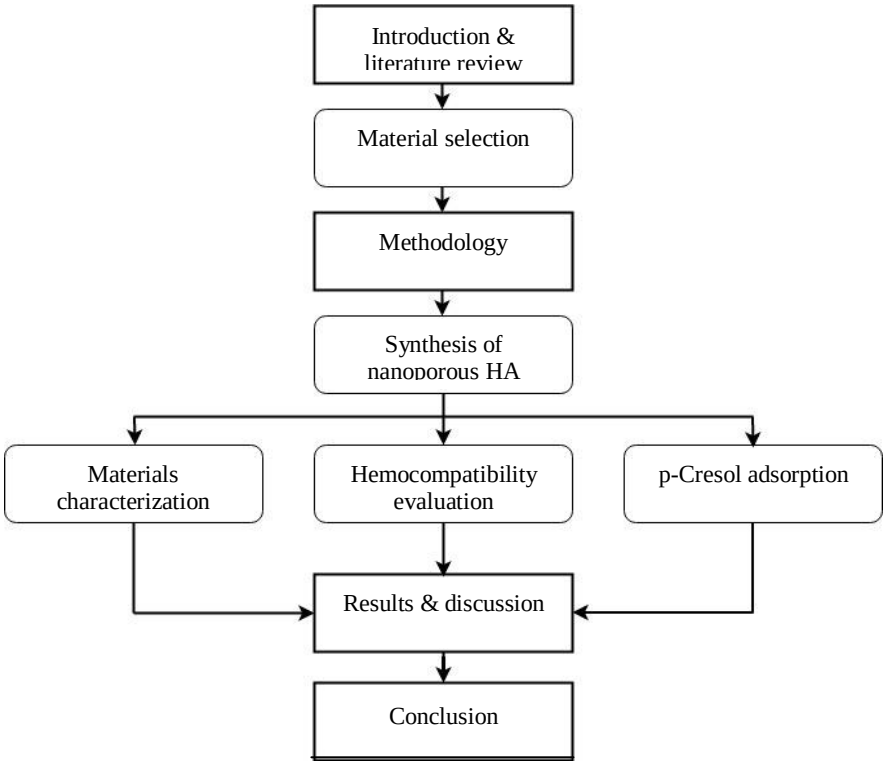

Figure 1.1 Project outline

CHAPTER 2

LITERATURE REVIEW

2.1 Human Kidney and its Function

Kidneys are a pair of bean-shaped organs (about 10-13 cm) located on either side of the spine, about the height of lower ribs and behind belly (Little, 2015). They play an important role in constantly filtrating blood and removing toxins. Kidneys can be classified into three main components such as cortex, medulla and renal pelvis as shown in Figure 2.1 (Dankers et al., 2011). Each kidney consists of one million of parallel mass transfer units, known as nephrons (Chabardes-Garonne et al., 2003). A nephron is made up of a glomerulus and encircled by a Bowman's capsule, which is linked to the proximal convoluted tubule, loop of Henle, distal convoluted tubule and collecting duct. Glomerulus and Bowman's capsule are a basic filtration unit in kidney, termed as renal corpuscle (Kriz and Elger, 2014). This unit eliminates filtrates especially uremic toxins, while important molecules such as glucose and amino acids are recovered through reabsorption by renal tubules (Dankers et al., 2011). Uremic toxins are accumulated at renal pelvis and excreted into ureter as urine.

Kidneys are natural filters in a human body which remove uremic toxins generated from metabolic activity via the discharge of urine. In addition to uremic toxins removal, kidneys are also responsible for maintaining the balance of salt, water, electrolytes such as calcium and phosphorus levels in the blood (Fissell et al., 2007). It involves in the control of acid-base balance in bodily fluids, regulating blood pressure, excretion of excess water as urine and production of hormones (e.g., erythroprotein for construction of red blood cells) (Stamatialis et al., 2008).

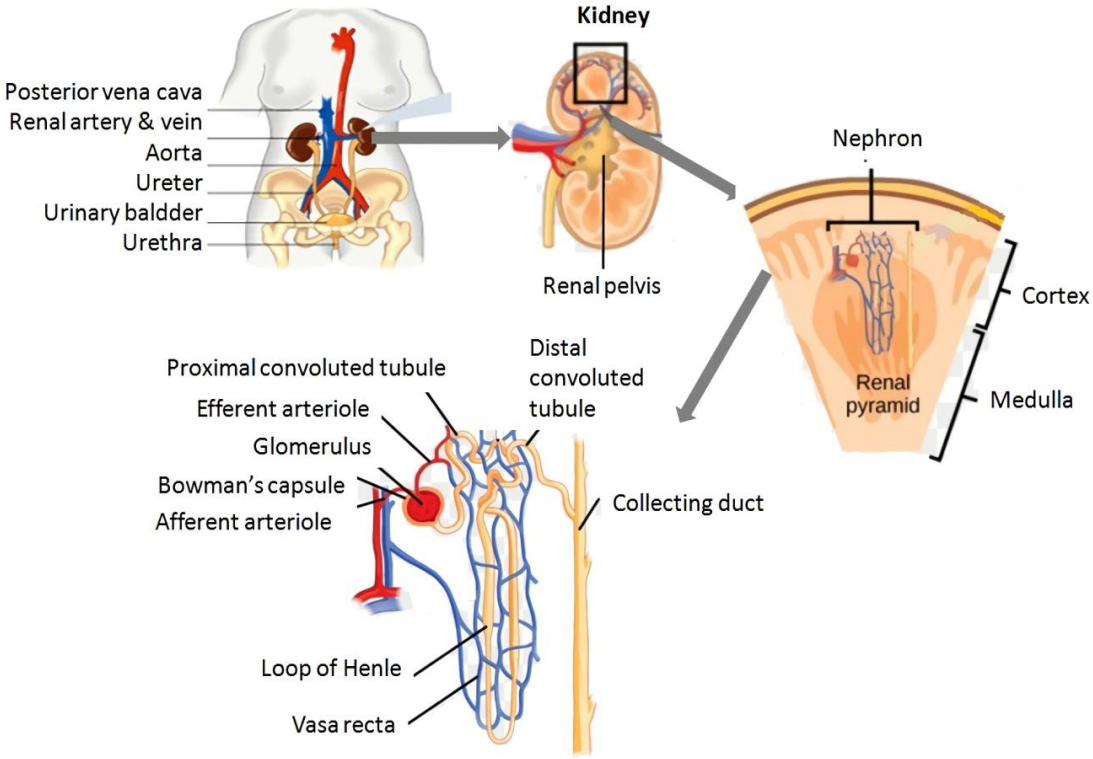

Figure 2.1 Schematic diagram of human kidney and nephron (modified from Nephron Kidney Glomerulus Renal Cortex Osmoregulation PNG, 2019)

2.1.1 Kidney Failure

Kidney damage or dysfunction could seriously affect a person's health and quality of life. It is important to understand the symptoms related to kidney failure, thus searching for the feasible solution to overcome its negative effects on the patients with kidney failure problem. The condition of partial or total loss of kidney function is known as kidney failure. Symptoms that indicate kidney dysfunction are an accumulation of uremic toxins and metabolic byproducts, increase in the water retention level and electrolyte shift in a body (Jèorres et al., 2010). Generally, kidney failure is categorized into two types, i.e., acute renal failure (ARF) and chronic kidney disease (CKD).

ARF is a condition where kidney loses it functions suddenly over a short period of hours to days. The symptoms for ARF are sudden increase of blood urea nitrogen (BUN), creatinine and electrolyte level in blood (Byham-Gray and Wiesen, 2004). On the other hand, CKD is an occurrence of progressive kidney damage over a period of months to years (Levey and Coresh, 2012). CKD is classified into five stages as shown in Table 2.1. CKD patients are normally facing the problem of decrease in kidney functionality or glomerular filtration rate (GFR), which indicates that the kidney is losing its functions to filter blood effectively. Glomerular filtration rate (GFR) is a measurement of the volume of blood passes through the glomeruli per minute. It is a common test to determine the stage of kidney failure suffered by patients.

Table 2.1 Stages of chronic kidney disease (Peter, 2007)

Stage	Detail	GFR (mL per minute per 1.73 m^2)
1	Kidney damage with normal kidney function	≥ 90
2	Kidney damage with mild loss of kidney function	60-89
3	Kidney damage with moderate loss of kidney function	30-59
4	Kidney damage with severe loss of kidney function	15-29
5	Kidney failure	< 15

* GFR = glomerular filtration rate
*Stage 5 is also termed as end-stage renal disease (ESRD)

Due to the complete failure of kidneys, patients suffering from Stage 5 CKD (end-stage renal disease, ESRD) have to undergo renal replacement therapy (RRT, e.g., kidney transplant, peritoneal dialysis and hemodialysis) to sustain their lives. Failure of receiving a renal replacement therapy would result in uremic toxins retention in a patient's body and eventually cause death (Davankov et al., 1997).

2.2 Uremic Toxins

Uremic toxins (sometimes is known as renal toxins) are wastes and byproducts generated from metabolism processes. The toxins are filtrated by kidneys and excreted from the human body via urination (Miyamoto et al., 2012). Uremia is a syndrome related to electrolyte imbalance and retention of uremic toxins in human body due to the kidney failure (Meyer and Hostetter, 2007). Uremic toxins are generally classified into three major groups based on their physicochemical properties. The three major groups are small water-soluble solutes, protein-bound solutes and middle molecules (Vanholder et al., 2003a). Small water-soluble solutes have a molecular weight of 500 Da (dalton, 1 Da = 1 g/mol) and below, while middle molecules possess molecular weight greater than 500 Da (Vanholder et al., 2003b).

The European Uremic Toxin (EUTox) Work Group has classified more than 90 known solutes as the uremic toxins found in the human body, they also provided the data on the concentrations of these solutes observed in healthy persons and ESRD patients (Meert et al., 2007, Duranton et al., 2012). The important uremic toxin information accessible from the data includes healthy human concentration (C_H), mean concentration of uremic toxins found in ESRD patients (C_U), maximal concentration (C_M) and reference sources. Table 2.2 shows several concentrations of major uremic toxins measured in healthy persons and ESRD patients. These data are crucial for identifying the sufficient amount of uremic toxins needs to be removed from ESRD patients' bodies by a renal replacement therapy.

Table 2.2 Concentrations of major uremic toxins measured in healthy persons and ESRD patients (Vanholder et al. 2003a; Vanholder et al. 2003b; Wernert et al. 2005)

Solute	C_H/ µM*	C_U/ µM*	C_M/ µM**	MW/ g/mol	Group
Small water-soluble					
Urea	< 6700	38333 ± 18333	76667	60	Carbamides
Creatinine	< 106	1204 ± 407	2124	113	Guanidines
Uric acid	< 400	496 ± 265	873	168	Purines
Protein-bound					
para-Cresol	5.6 ± 9	186 ± 41	377	108	Phenols
Indoxyl sulfate	2.4 ± 22	211 ± 365	940	251	Indoles
Middle molecule					
B_2-microglobulin	< 0.17	4.7 ± 0.7	8.5	11818	Peptides
Leptin	0.001	0.01	0.03	16000	Peptides

C_H = Healthy human concentration
C_U = Mean Uremic concentration
C_M = Maximal uremic concentration
MW = Molecular weight
* Values are presented as means ± SD
** Values are presented as medians

The data by EUTox Work Group reveals that the concentrations of small water-soluble solutes (i.e., urea, creatinine and uric acid) measured in ESRD patients' body are relatively high as compared to the protein-bound solutes and middle molecules. Hence, the present renal replacement therapies are focusing on the removal of small water-soluble solutes. Urea and creatinine are used as markers for assessing the dialysis adequacy received by ESRD patients (Waniewski et al., 2006, Pandya et al., 2016). However, the focus on the removal of small water-soluble solutes in renal replacement therapy is incapable to help ESRD patients to restore their health due to the retention of other uremic toxins, particularly protein-bound solutes (i.e., *para*-cresol).

para-Cresol (*p*-cresol) is one of the uremic toxins categorized under the protein-bound solutes. It is a waste generated from the protein metabolic process in the human gastrointestinal system, which is normally eliminated from a body via urination and defecation (Vanholder et al., 1999). *p*-Cresol is an organic compound with the formula $CH_3C_6H_4(OH)$, its other physical properties are shown in Table 2.3.

Table 2.3 Physical properties of *p*-cresol (ATSDR 2008; Wernert et al. 2005)

Property	Detail
Chemical name	*para*-Cresol, 4-methylphenol
Chemical formula	$CH_3C_6H_4(OH)$
Molecular weight	108 g/mol
Melting point	35 ˚C
Boiling point	202 ˚C
Appearance	Colourless
Density	1.03 g/mL (at 25 ˚C)
Odor	Phenol-like
Solubility	Water: 20 g/L (25 ˚C) Ethanol: fully miscible Diethyl ether: fully miscible
Size of molecule (nm)*	x: 0.66 y: 0.76 z: 0.39
Chemical structure	

* The size of *p*-cresol molecule was estimated using Cerius^2 software by Wernert and co-workers (2005)

p-Cresol is a partially lipophilic solute which easily binds to protein (Dou et al., 2002). It appears as both protein-bound solute and free solute (non-protein bound) in ESRD patients' bodies (Concentrations of the solutes are presented in Table 1.1) (Bammens et al., 2006). Studies by nephrologists revealed that *p*-cresol molecules (protein-bound and free solutes) are greatly accumulated in ESRD patients' bodies even though undergoing renal replacement therapy. Its concentration is about 32 times higher than that of healthy persons (Vanholder et al., 2003a, Lin et al., 2011).

The retention of the *p*-cresol molecules in ESRD patients could result in very harmful effects, i.e., inhibition of platelet activating factor synthesis (Wratten et al., 1999), decrease in the response of activated polymorphonuclear leukocytes (Vanholder et al., 1995) and reduction of endothelial cell response to inflammatory cytokines (Dou et al., 2002). Recent findings show that the accumulation of free *p*-cresol molecules is associated with mortality (Bammens et al., 2006) and increased the risk of ESRD patients to have cardiovascular disease (Meijers et al., 2008). Judging from the possible occurrence of such serious problems, it is vital to remove the *p*-cresol as compared to small water-soluble solutes which are mere uremic markers.

2.3 Artificial Kidney

Renal replacement therapy is an important treatment for ESRD patients to eliminate uremic toxins from their bodies. At present, the therapies that are favoured options to the ESRD patients are kidney transplant, peritoneal dialysis and hemodialysis (Figure 2.2). Hemodialysis remains the highest utilized renal replacement therapy. These therapies have different working principles in removing uremic toxins and they are often synonymous with the term artificial kidney (except kidney transplant).

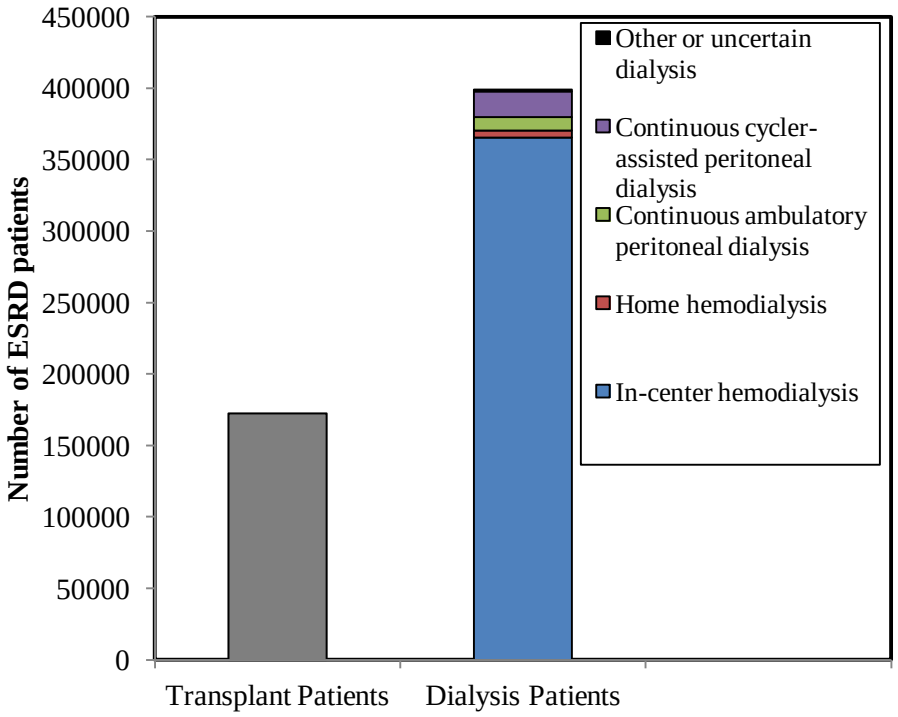

Figure 2.2 ESRD treatment modality (Health, 2011)

Kidney transplant is a process of placing a healthy kidney from a live or deceased person into an ESRD patient to filtrate the blood. This process can be categorized as deceased-donor (kidney obtained from a recent dead body) or living-donor transplant depending on the source of the organ. Only one donated kidney is required to replace two dysfunctional kidneys, making the living-donor kidney transplant a preferred option to ESRD patients. This would significantly improve the ESRD patient's health and quality of life. One of the major challenges in this process is the limited amount of healthy kidneys available for the ESRD patients. The donor-recipient compatibility of the organ and other medical complications are affecting the survival of the patients receiving the treatment (Hariharan et al., 2002, Sellares et al., 2012).

Peritoneal dialysis uses a patient's peritoneum in the abdomen as a membrane to remove uremic toxins and excess fluid from the blood (Figure 2.3). Before

receiving a peritoneal dialysis, a soft tube, known as a catheter is placed in an ESRD patient's belly. During the dialysis treatment, dialysate flows from a bag through the catheter into an ESRD patient's belly. Uremic toxins and excess fluid diffuse through the peritoneum into the dialysate until it reach equilibrium with the body's fluid. The used dialysate is then drained into an empty bag and replaced with fresh dialysate (Nolph and Twardowski, 1989). It is a home based dialysis treatment for ESRD patients that offer better mobility and lower cost. However, the peritoneal dialysis is inefficient in removing protein-bound uremic toxin, i.e., *p*-cresol. About 38.1 % of *p*-cresol is removed by the peritoneal dialysis which is relatively low compared to urea (68.4 %) and it could induce harmful effects to dialysis patients (as mentioned in Section 2.2) (Thiery et al., 2018). This treatment is highly correlated with the risk of infection (Li et al., 2010) and peritoneal membrane loss over dialysis duration (Baroni et al., 2012). Although peritoneal dialysis shows higher survival rate during the initial stage of dialysis (first three months), the rate drop drastically after a longer treatment period (two years) as compared to the hemodialysis (Sinnakirouchenan and Holley, 2011, Thiery et al., 2018).

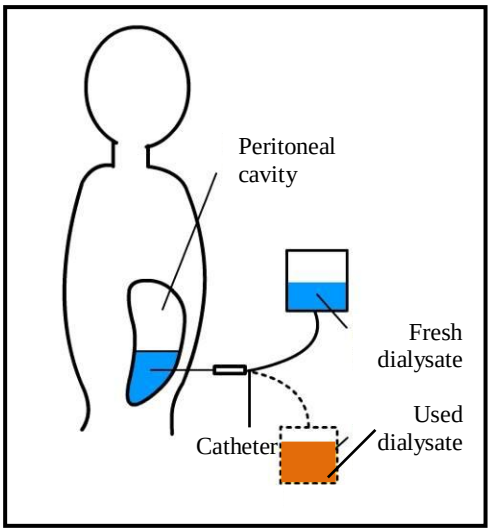

Figure 2.3 Schematic diagram of peritoneal dialysis

Due to the limited amount of healthy kidneys available for organ transplant and high infection risk of peritoneal dialysis, hemodialysis still remains the most viable option in terms of treatment efficiency, safety and cost. A study by Thiery and co-workers (2018) shows that the median survival times for ESRD patients receiving hemodialysis and peritoneal dialysis are 53.5 and 38.6 months, respectively, indicating that the hemodialysis is a better treatment for the patients. Hemodialysis is a process of removing uremic toxins from an ESRD patient's blood through semipermeable membranes into a dialysate. Hemodialysis treatment can be carried out in a dialysis center, hospital or at home. During the treatment, a patient will be connected to a dialysis machine for about 4 hours and the procedure is repeated three times per week (Finkelstein et al., 2012). Thus, specialized staffs such as nurses and technicians are assigned to handle the dialysis patients during the treatment.

2.3.1 Hemodialysis

During hemodialysis treatment, two needles are placed into a patient's arm to flow his/her blood into a dialyzer for filtrating uremic toxins. A peristaltic pump circulates the blood over a semipermeable membrane inside a dialyzer in one direction while dialysate is flowed in an opposite direction, which is known as counter-current flow. The uremic toxins in the blood pass through semipermeable membrane and flow to dialysate due to the concentration gradient (Cameron, 1996). The schematic diagram of a hemodialysis system and dialyzer are shown in Figure 2.4 and 2.5, respectively.

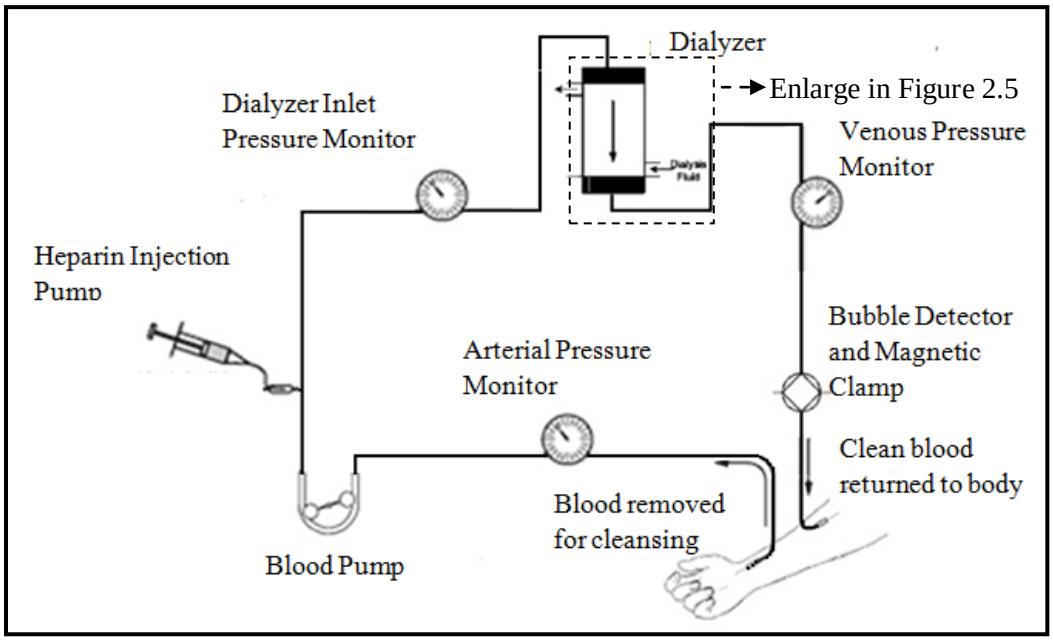

Figure 2.4 Schematic diagram of a present hemodialysis (Jèorres et al., 2010)

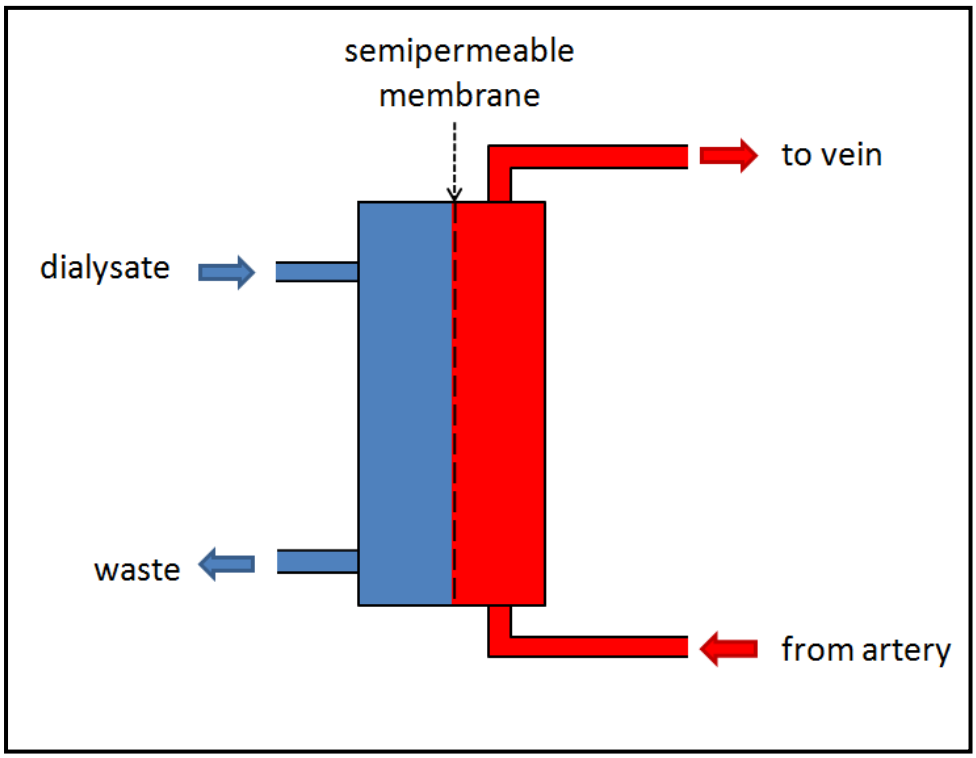

Figure 2.5 Schematic diagram of a dialyzer

A hemodialysis machine is generally made up of peristaltic pumps, dialyzer and detectors. It constantly measures the blood pressure, flow rate, amount of fluid removal and other important information when an ESRD patient is receiving hemodialysis treatment. Nurses and doctors rely on the information to determine the dialysis adequacy received by an ESRD patient. Purified water is mixed with acid and basic concentrates in the hemodialysis machine to prepare the dialysate. Presently, there are several manufacturers producing hemodialysis machine, i.e., Fresenius Medical Care, Gambro, Nikkiso, B Braun, Toray and Nipro (Polaschegg et al., 2010). Figure 2.6 shows a dialyzer (model F8HPS, polysulfone membrane) manufactured by Fresenius Medical Care.

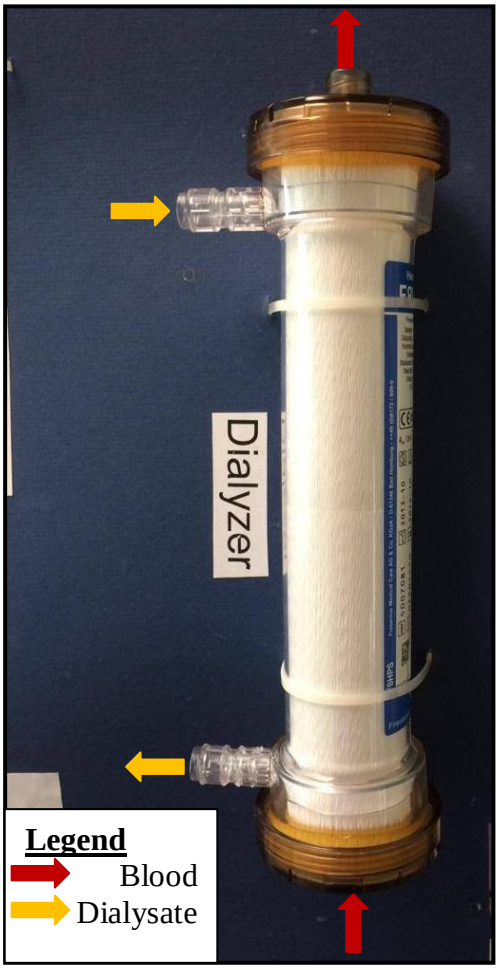

Figure 2.6 Dialyzer used in a hemodialysis treatment (Fresenious Medical Care)

2.3.1(a) Dialyzer

A dialyzer is made up of semipermeable membranes which have a certain range of pore size (ranging from 1 to 100 nm) to allow uremic toxins to diffuse from a patient's blood into the dialysate, while plasma and blood cells remain in the blood (Yang et al., 2007). Conventional hemodialysis system used cellulose membranes based dialyzer for filtrating toxins but it is only capable of removing small water-soluble solutes effectively (Kee and Idris, 2010). In recent years, synthetic polymers such as polysulfone, polyethersulfone, polycarbonate, polyamide and polyacrylonitrile are used in a dialyzer for the blood filtration (Gao et al., 2014, Abe et al., 2017). These synthetic polymers are 10 times more permeable and efficient in removing middle molecules as compared to the cellulose membranes (Gao et al., 2014).

The synthetic polymers based membranes that contain small pore size are termed as low-flux, while those with large pore size are known as high-flux (Yang et al., 2007). Both low and high-flux membranes are effective in removing small water-soluble solutes such as urea, uric acid and creatinine. A high-flux membrane which contains larger pores allows more uremic toxins, especially middle molecules to diffuse from ESRD patients' blood into the dialysate (Oshvandi et al., 2014). Hence, it is commonly used in hemodialysis treatment to improve the dialysis adequacy received by ESRD patients. The dialyzer is replaced after several uses (a dialyzer is used three times in hemodialysis treatment for an ESRD patient) to maintain the dialysis efficiency and prevent contamination.

2.3.1(b) Dialysate

Dialysate is generally made up of purified water, sodium chloride, sodium bicarbonate or sodium acetate, calcium chloride, potassium chloride, magnesium

chloride and glucose (Tong et al., 2001). It is used in the hemodialysis process to promote the uremic toxins removal, maintains the electrolytes and acid-base balance in a dialysis patient's body. Water is the main component of the dialysate and it needs to be purified to prevent disease or poisoning to dialysis patients.

The water used for preparing dialysate has to undergo a series of treatments to eliminate impurities such as bacteria, metals, mud and chemicals. The treatments involved in the water purification are pretreatment filtration, softeners, carbon beds, reverse osmosis systems, ultraviolet irradiators, endotoxin filters and chlorine regulation processes (Ronco and Cruz, 2008). A pipeline system is constructed to flow purified water from a storage tank into a hemodialysis machine and mix with concentrates (acid and basic) during dialysis treatment (Desai, 2015). Specialized technicians are required to monitor the water treatment and dialysate preparation regularly in a designated area inside dialysis centers or hospital; this complicated the dialysis process and increased the operating cost.

2.3.1(c) Limitation of Hemodialysis

Hemodialysis is a preferable treatment for ESRD patients due to its relatively high capability of removing uremic toxins (i.e., small water-soluble solutes and middle molecules) and low infection risk as compared to the other renal replacement therapies. However, the hemodialysis system is inefficient in removing protein-bound uremic toxins, particularly *p*-cresol. The large molecular size and agglomeration with protein have impeded the effective removal of the *p*-cresol from an ESRD patient's body through the semipermeable membrane in a dialyzer (Brunet et al., 2003). Many attempts have been made to improve the protein-bound uremic toxins removal adequacy such as constant use of high-flux dialyzer, prolong the dialysis duration,